

Article

Effect of Coarse Recycled Aggregate on Failure Strength for Asphalt Mixture Using Experimental and DEM Method

Yongsheng Yao ¹, Jue Li ^{1,*} , Chenghao Liang ² and Xin Hu ²

¹ College of Traffic & Transportation, Chongqing Jiaotong University, Chongqing 400074, China; yaoyongsheng23@163.com

² School of Civil Engineering, Central South University of Forestry and Technology, Changsha 410004, China; liangchenghao@csuft.edu.cn (C.L.); hxdgrwnbybz@163.com (X.H.)

* Correspondence: lijue1207@cqjtu.edu.cn

Abstract: Coarse aggregate is the major part of asphalt mixture, and plays an essential role in mechanical performance of pavement structure. However, the use of poor-quality coarse recycled aggregate (CRA) reduces the strength and stability of the aggregate skeleton. It is a challenge to predict accurately the influence of CRA on the performance of asphalt mixture. In this study, both a uniaxial compression test and a direct tensile test were carried out to evaluate the failure strength of asphalt concrete with four CRA content. The discrete element method (DEM) was applied to simulate the specimen of asphalt concrete considering the distribution and properties of CRA. The results showed that temperature and loading rate have a significant influence on failure strength, especially when the CRA content was more than 20%. With the increase of CRA content, both cohesion force and internal friction angle were gradually weakened. The proposed model can be used to predict the failure strength of asphalt mixture, since both experimental and simulated results had a high consistency and repeatability. With the decrease of CRA strength, the nominal cohesion force of the specimen decreased, while the internal friction angle increased.

Keywords: asphalt mixture; recycled aggregate; failure strength; uniaxial compression test; direct tensile test; discrete element method



Citation: Yao, Y.; Li, J.; Liang, C.; Hu, X. Effect of Coarse Recycled Aggregate on Failure Strength for Asphalt Mixture Using Experimental and DEM Method. *Coatings* **2021**, *11*, 1234. <https://doi.org/10.3390/coatings11101234>

Academic Editor: Andrea Nobili

Received: 12 September 2021

Accepted: 8 October 2021

Published: 11 October 2021

Publisher's Note: MDPI stays neutral with regard to jurisdictional claims in published maps and institutional affiliations.



Copyright: © 2021 by the authors. Licensee MDPI, Basel, Switzerland. This article is an open access article distributed under the terms and conditions of the Creative Commons Attribution (CC BY) license (<https://creativecommons.org/licenses/by/4.0/>).

1. Introduction

The recycling of construction and demolition (C&D) materials have attracted much attention in pavement engineering because of its huge environmental and economic benefits [1]. With the development of cities, a large number of C&D wastes have been produced, resulting in more and more land occupation and pollution [2]. On the other hand, since pavement construction consumes a large amount of sand and gravel, the potential utilization rate of C&D waste is very high for pavement materials. This is a sustainable way to solve the over exploitation of mine resources, by crushing C&D waste into recycled aggregate (RA) instead of natural aggregate. The recovery rate of C&D was as high as 95% in developed countries, while only about 5% of C&D waste was recovered in China [3]. Therefore, the recycling of C&D waste in pavement engineering has broad application prospects and economic value.

It is commonly believed that, due to the high proportion of coarse recycled aggregate in the mixture, this replacement will have different effects on the physical or mechanical properties of asphalt mixture [4]. Compared with natural materials, RA has some defects, such as additional impurities and lower strength. After crushing, the RA has a rough surface and more cracks [5]. When the particle size of RA is larger than 19 mm, it does not meet the technical requirements of pavement engineering, such as low crushing value [6]. Fatemi et al. [7] found that the addition of RA could change the optimal binder content and maximum bulk density of asphalt mixture. Some recent studies have implied that the asphalt mixture has higher high temperature stability than the mixture without RA,

because the addition of RA changes the void ratio and surface contact of the asphalt mixture [8,9]. Its low temperature stability, water stability and durability were worse than that without RA [10]. In conclusion, the strength of RA is weaker than that of natural aggregate, and the contact performance between asphalt mastic and aggregate needs to be further improved [11]. Obviously, the content and properties of RA are important factors affecting the service performance of asphalt mixture. The application of recycled aggregate in asphalt mixture has become a challenge, along the premise of ensuring performance.

Under the action of traffic load and environmental factors, asphalt mixture experiences large unrecoverable deformation, which even causes the failure of pavement structure [12,13]. Current research has mainly evaluated the failure strength of asphalt mixture through laboratory tests, such as the uniaxial compression test, direct tensile test, semi-circular bending test, etc. [14–16]. Qin et al. [17] found that the dynamic modulus curve under indirect tension was lower than that under uniaxial tension, which depends on temperature and loading frequency. Cerni et al. [18] suggested that there was good correlation between dynamic modulus and indirect tensile modulus of asphalt mixture at different temperatures. Lv et al. [19] compared the fatigue test results under different conditions and proposed a unified modulus calculation method. Meanwhile, some studies have shown that the mechanical properties of the asphalt mixture were also related to factors such as the spatial location of the specimen components [20] and the compaction method [21]. However, since both strength and location of coarse aggregates are distributed randomly in natural state, the current experimental methods (or packing theory) are not capable of quantitatively characterizing the effect of aggregate properties on the failure strength of asphalt mixture.

To solve this issue, the discrete element method (DEM) and the X-ray CT technology have been increasingly utilized for evaluating the internal structure of asphalt mixture in current studies. Shaheen et al. [22] applied an X-ray CT device to evaluate fatigue cracking by capturing the arrangement of air voids. Chen et al. [23] suggested that the DEM provided a helpful way to analyzing the compacting behavior of asphalt mixture, and its simulation was in good agreement with that of the X-ray CT scan in air void distribution. Although capturing the 3D air-void structure based on the X-ray CT has been well researched, simulating the heterogeneity of aggregates remains problematic. The X-ray CT detection needs professional technicians and expensive equipment, and the stacked aggregates within asphalt mixture cannot be distinguished accurately by the image threshold. With the advantages of granular materials, the DEM is potentially efficient to deal with the distribution and packing of aggregates [24]. Recently, the asphalt mixture is usually simplified in DEM and made up by a lot of spherical particles as basic computing elements, which follow Newton's second law of motion [25]. Past studies have demonstrated that these simplified models could describe well the packing structure in coarse aggregates larger than 2.36 mm, and match the experimental data of mechanical properties successfully [26–28]. Additionally, Feng et al. [29] reported that the DEM is a valuable contact model to characterize the viscoelastic behavior of asphalt mixture in normal and shear conditions. Therefore, the DEM approach was used in this study to predict the failure strength of asphalt mixture using coarse recycled aggregate.

The purpose of this study is to reveal the influence of Coarse RA (CRA) on the failure strength of asphalt mixture using experimental and numerical tests. The uniaxial compression test and direct tensile test were carried out to obtain mechanical performances for asphalt mixture. According to the Mohr-Coulomb theory, the failure strength of asphalt mixture was calculated, including the cohesive force c and the friction angle φ . Additionally, a numerical simulation was proposed to investigate the influence of CRA properties on the strength of asphalt mixture using DEM. This paper is divided into four parts. The following section mainly introduces the physical properties of materials and test procedures in the laboratory and in DEM simulation. Then the testing results and their influencing factors are analyzed. Through the change of failure strength, the influence mechanism of recycled coarse aggregate on the performance of asphalt mixture is explained. Furthermore, in order to evaluate the influence of CRA properties on the performance of asphalt mixture, a DEM

model is established and tested. Finally, the main findings of this research are discussed and summarized.

2. Materials and Methods

2.1. Materials

The aggregates tested in this study are limestone and RA. Limestone is used as the fresh aggregate and RA as the secondary aggregate. The chemical composition of natural limestone is shown in Table 1. The RA mainly consists of broken bricks and concrete, as shown in Figure 1. In the process of crushing, some micro-cracks appeared on the surface of RA particles, which resulted in the decrease of aggregate strength and the increase of voids. At present, due to the manufacturing process, there are more particles below 0.075 mm in RA. These fine particles not only have the characteristics of light weight and low strength, but are also often coated on the RA surface, which affects the combination of aggregate and asphalt binder. Therefore, only the CRA larger than 2.36 mm was retained by mesh screening and water washing and the dust particles were removed.

Table 1. Chemical components of limestone.

| CaO | SiO ₂ | Al ₂ O ₃ | Fe ₂ O ₃ | Other |
|-------|------------------|--------------------------------|--------------------------------|-------|
| 57.85 | 24.03 | 4.37 | 1.19 | 12.56 |



Figure 1. Recycled aggregates from C&D materials.

The relevant physical properties of aggregates are shown in Table 2. The water absorption of CRA was much greater than that of fresh aggregate due to its high surface porosity. Additionally, the abrasion strength of CRA was slightly less than the limit value of standard ASTM, as mentioned in previous studies [30]. However, its mix with limestone aggregate could compensate for these defects of CRA including the high water absorption and the weak strength. To obtain a satisfactory testing aggregate, Martinho et al. [6] suggested that it was common in asphalt mixture that the application of CRA in content of around 35% allowed a mechanical performance of aggregate mixture similar to that of the fresh aggregate.

Table 2. Physical properties of aggregates.

| Properties | Fresh Aggregates | Secondary Aggregates | Standard ASTM | Requirements |
|-----------------------------------|------------------|----------------------|---------------|--------------|
| Coarse aggregate | | | | |
| Bulk specific gravity | 1.68 | 1.47 | C127 | — |
| Apparent specific gravity | 2.73 | 2.59 | C127 | — |
| Los Angeles abrasion (%) | 17.4 | 27.3 | C131 | ≤25 |
| Percentage of fractured particles | 93 | 87 | D5821 | ≥90 |
| Water absorption (%) | 0.75 | 5.80 | C127 | ≤2.5 |
| Fine aggregate | | | | |
| Bulk specific gravity | 1.59 | — | C128 | — |
| Apparent specific gravity | 2.71 | — | C128 | — |
| Sand equivalent (SE) | 69 | — | D2419 | ≥50 |
| Water absorption (%) | 1.90 | — | C128 | ≤2.5 |

In all tested asphalt mixtures, 70 penetration bitumen was used as the binder. In order to characterize the performance of asphalt binder, regular performance tests were carried out, such as softening point evaluation, penetration and ductility test. The performance test results of base asphalt are shown in Table 3.

Table 3. Performance test results of 70 penetration bitumen.

| Properties | Values | Standard ASTM | Requirements |
|--|--------|---------------|--------------|
| Density at 15 °C (gr/cm ³) | 1.032 | D7076 | — |
| Softening point (R&B °C) | 47 | C3676 | ≥46 |
| Penetration at 25 °C (0.1 mm) | 70 | D573 | 60~80 |
| Ductility at 15 °C (cm) | 123 | D11379 | ≥100 |
| Flash point (°C) | 275 | D9278 | ≥260 |
| Dynamic viscosity at 60 °C (Pa·s) | 216 | D2171 | ≥180 |

2.2. Mixture Design

In this study, the gradation of hot-mix asphalt mixture (HMA) was selected by the average value for the limit of dense aggregate gradation recommended by ASTM specification, as shown in Figure 2. The maximum particle size of aggregates is 19.0 mm. Both CRA and flesh aggregate were mixed on each sieve larger than 2.36 mm according to the target size gradation. The fine aggregate was included only for limestone. Four levels of CRA addition (10%, 20%, 30% and 40% by weight) were tested in the recycled HMA. Moreover, the mixture made up of pure fresh aggregates was also tried as a control.

Marshall mix design procedures were performed by ASTM D1559 to obtain the optimum asphalt content for the HMA containing 20% wt% CRA and 80% wt% limestone coarse aggregate. Three similar specimens, whose asphalt content varied from 3.5% to 6.5% in increments of 0.5%, were prepared by the Marshall compaction. The mixture was poured into the cylindrical mold and hammered by 75 times to each side. The optimum asphalt content was determined as 5.6% by meeting the maximum unit weight and 4% air voids. Considering the aim of this study, all HMA specimens were made by the same asphalt content of 5.6%.

2.3. Experimental Methods

Uniaxial compression tests and direct tensile tests were carried out in this study, using the MTS810 material testing machine (MTS Systems Corporation, Eden Prairie, MN, USA). The slab specimen was compacted at 16 passes by a compacting roller with a maximum pressure of 0.9 MPa [31]. Its size was 300 mm by 300 mm in plan and 50 mm in height. After the preparation of slab specimens, a series of prismatic specimens were cut along

the rolling direction. The size of the uniaxial compression specimen is 40 mm × 40 mm × 80 mm, while that of the direct tension specimen is 40 mm × 40 mm × 60 mm.

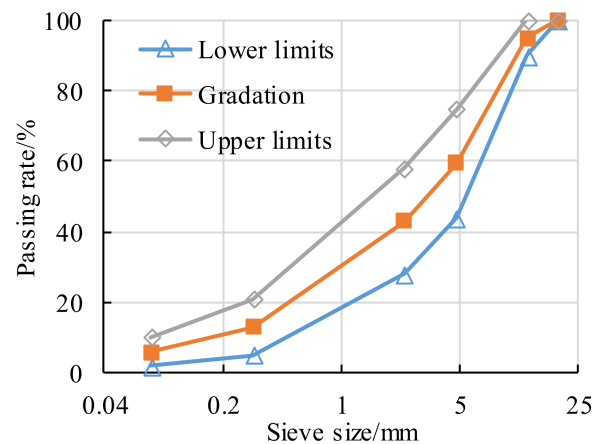


Figure 2. Size gradation of aggregates.

2.3.1. Uniaxial Compression Test

The uniaxial compression test is one of the typical methods to determine the strength characteristics of asphalt mixture. It has the characteristics of simple operation and good economy. Some researchers have tried to establish a DEM model for the uniaxial test of asphalt mixtures, and use the axial stress-strain to calibrate the parameters. At different temperatures, the resilient modulus and compressive strength of the asphalt mixture will change significantly because its viscoelastic characteristics depend on temperature.

The uniaxial compression test of asphalt mixture was carried out according to the Chinese standard [31]. Meanwhile, different temperatures and loading rates were considered in this study. As for compression failure, its strength increases sharply with the decrease of temperature. Therefore, based on the preloading results, the test temperatures were determined to be 10, 20, 40 and 60 °C, respectively. The MTS810 material testing machine was used to load the specimen, and five loading rates were adopted: 1.0, 2.0, 4.0, 8.0 and 16.0 cm/min.

2.3.2. Direct Tensile Test

The direct tensile test is mainly used to evaluate the low-temperature crack resistance of asphalt mixture. According to the standard [31], the tensile tests were carried out on asphalt mixture at 10, 20, 40 and 60 °C, respectively, and load-time curves were measured at rates of 1.0, 2.0, 4.0, 8.0 and 16.0 cm/min. The mold and specimen were bonded through epoxy resin and cured at room temperature for 24 h. Then, the specimen was placed in a low-temperature chamber to lower to the test temperature, which took about 4 h.

2.3.3. Time Temperature Equivalence Principle

As a viscoelastic material, the mechanical properties of asphalt mixture are related to the temperature and loading time [32,33]. Under different temperature and loading frequency, asphalt mixture may present the same mechanical properties, which is called the time temperature equivalence principle. According to this principle, in the logarithmic coordinate system mechanical parameters at different temperatures are translated to the reference temperature, and a smooth curve can be obtained, which is the main curve at the reference temperature.

2.3.4. Mohr-Coulomb Theory

The mechanical properties of asphalt mixtures are affected by aggregate properties and stacking structure because of their granular properties. The strength composition of

asphalt mixture includes the cohesive force generated by asphalt and the inner frictional resistance generated by aggregate. It is generally believed that the Mohr Coulomb model can describe well the strength characteristics of materials, as shown in Equation (1) [34].

$$f = \sigma_1 - \sigma_3 - (\sigma_1 + \sigma_3) \sin \varphi - 2c \cos \varphi = 0 \quad (1)$$

where σ_1 and σ_3 are the maximum and the minimum principal stresses; c stands for the cohesive force; and φ stands for the internal friction angle.

The compressive strength R_c and tensile strength R_t of the specimen when it is broken can be determined by laboratory tests. For the unconfined compression condition, the confining pressure of the specimen is 0, which is the minimum principal stress $\sigma_3 = 0$. For direct tensile conditions, the maximum principal stress σ_3 is 0, and the minimum principal stress σ_1 is $-R_t$. Therefore, by substituting parameters R_c and R_t into Equation (1), the cohesive force c and the internal friction angle φ can be calculated, as shown in Equations (2) and (3). It is assumed that the parameter values of asphalt mixture under tensile and compression tests are the same.

$$\varphi = \arcsin\left(\frac{R_c - R_t}{R_c + R_t}\right) \quad (2)$$

$$c = \frac{1}{2}\sqrt{R_c R_t} \quad (3)$$

2.4. Numerical Simulation

Based on the results of laboratory tests, further studies were carried out to reveal the influence mechanism of C&D materials on the uniaxial failure of asphalt mixture under the microstructure. The 3D DEM model was established to simulate the test specimens of asphalt mixture, although the established method was also applicable to other asphalt mixtures [35]. For aggregate particles, a group of spherical particles with different particle sizes were used in this DEM simulation to replace aggregates. The size of the digital aggregate follows the particle size distribution shown in Figure 2. The DEM model is shown in Figure 3.

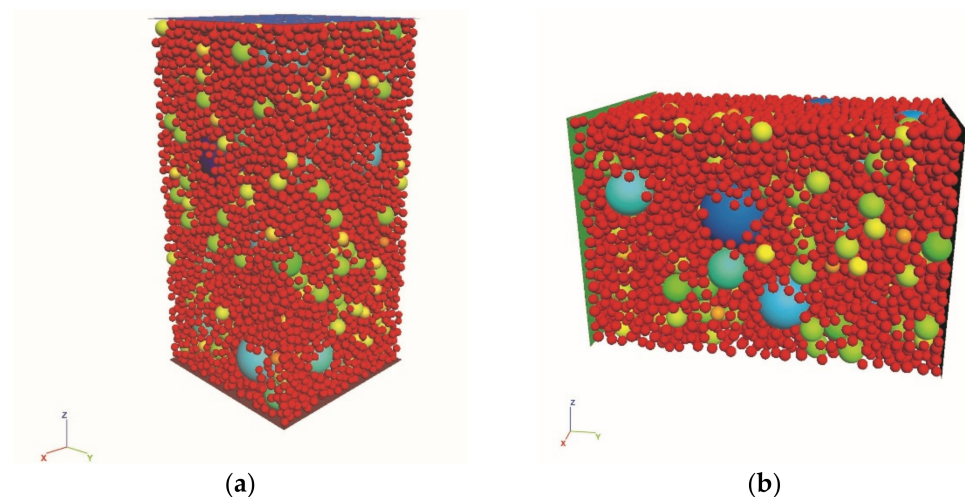


Figure 3. DEM models of the asphalt mixture for: (a) uniaxial compression; (b) direct tensile.

The specimen of asphalt mixture is composed of aggregate, asphalt mastic and porosity. In the DEM, the use of spherical particles can simplify the calculation process of asphalt mixture, so as to save calculation time and memory capacity. At the same time, it is generally believed that fine particles with size less than 2.36 mm have little influence on the test results, so spherical particles with unified particle size were used as asphalt mastic.

The random distribution of aggregate results in the non-uniformity of microstructure in the sample. The DEM has two important calculation links, i.e., displacement equation and motion equation. The normal and tangential contact forces were determined by the contact displacement between the two units, which meets the requirements of Equations (4) and (5).

$$F_n = K_n \times U_n \quad (4)$$

$$\Delta F_t = -K_t \Delta U_t \quad (5)$$

where F_n is the normal contact force; F_t is the tangential contact force; K_n and K_t are the stiffness in the normal and tangential directions, respectively; U_n is the normal displacement; and ΔU_t is the tangential displacement increment.

On the other hand, the motion of all units follows Newton's equations of motion. The translation and rotation of each unit were determined by the unbalanced force and torques acting on the unit. Therefore, the motion law of each element at any time should meet the balance law of translational motion and rotation of a rigid body.

It was necessary to determine the contact form of internal materials and the selection of contact model in the process of specimen generation. There were three main contact forms in the numerical specimen: (1) contact between adjacent aggregate particle clusters; (2) internal unit contact action of asphalt mastic; (3) contact between asphalt mastic and aggregate. The contact model is used to describe the mechanical action inside materials and between them. For the assignment of contact models, it was assumed that the contact parameters between coarse aggregate and asphalt mastic are consistent with those between internal units of asphalt mastic. Since the stiffness and friction coefficient of recycled aggregate were variable, Gauss was used to randomly generate the stiffness and friction coefficient of RA. Among them, the initial stiffness of RA was set as half of the strength of the fresh aggregate. Burgers model built in PFC5.0 software was applied to describe the viscoelastic characteristic of asphalt mastic [21]. Therefore, the contact between aggregates was described by a linear model, and the contact model of asphalt mastic by Burgers model. All contact parameters were calibrated with laboratory test results, by repeatedly adjusting the parameters to make the simulation curve close to the test results. The mechanical parameters after calibration are shown in Table 4.

Table 4. Contact models and parameters at 20 °C.

| Properties | Values |
|----------------------------------|-------------------|
| Linear model for aggregates | |
| Effective modulus (Pa) | 6.0×10^7 |
| Stiffness ratio | 2.4 |
| Friction coefficient | 0.17 |
| Burgers model for asphalt mastic | |
| Stiffness of Kelvin (Pa) | 3.5×10^6 |
| Viscosity of Kelvin (Pa·s) | 4.3×10^4 |
| Stiffness of Maxwell (Pa) | 6.3×10^6 |
| Viscosity of Maxwell (Pa·s) | 5.4×10^5 |
| Bond strength (Pa) | 1.2×10^6 |
| Stiffness ratio | 1.0 |

3. Results

3.1. Experimental Investigations

3.1.1. Uniaxial Compression Test

Figure 4 displays the uniaxial compression test results of asphalt mixture with different CRA content at 20 °C. As an example, the preset loading rate of these tests is 4min/min. The change trend of the loading curve can be divided into three processes, i.e., elastic stage, inelastic yield stage and failure stage. Firstly, the mechanical behavior at this stage

was dominated by elasticity, and the loading curve had a linear growth; the curve in the inelastic stage displayed a nonlinear change. During this process, the material has a certain yield state, and the slope of the curve gradually decreases to zero, which is the peak of the load. After that, the stress decreased rapidly until the asphalt mixture specimen completely failed. Therefore, the asphalt mixture has a similar failure behavior with different CRA content, gradually changing from the elastic zone in the initial stage to the inelastic yield zone, and was destroyed quickly after reaching the peak.

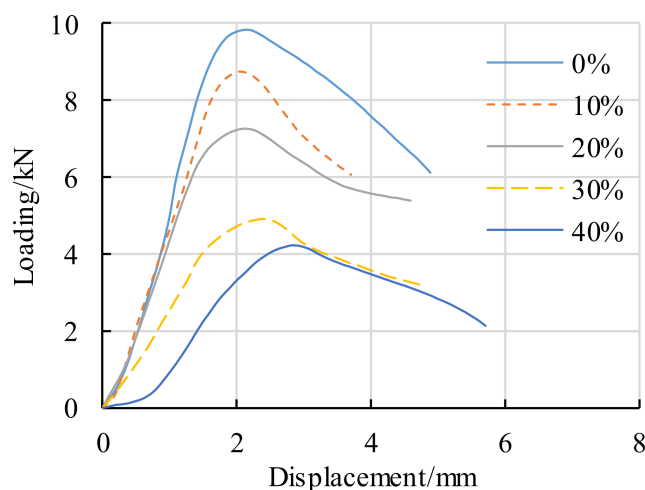


Figure 4. Loading to displacement curves of uniaxial compression tests.

In addition, the results in Figure 4 also showed that with the increase of CRA content, the failure peak of asphalt mixture decreases and the displacement required for failure increases. The compressive strength and the compression stiffness modulus were used in this study to quantify the failure behavior of asphalt mixture. The definitions of the two parameters were shown in Equations (6) and (7). Since the axial strain corresponds to the displacement in the test, the stiffness modulus can characterize the ability of the specimen to resist deformation in the elastic stage.

$$R_c = \frac{P_c}{bl} \quad (6)$$

$$S_c = \frac{R_c}{\varepsilon_c} \quad (7)$$

where P_c is the maximum loading at failure; b and l are the width and the length of specimens; and ε_c is the axial strain.

Figure 5 shows the failure performance of asphalt mixture mixed with 20% CRA at different temperatures and loading rates. At different temperatures, the failure strength of the asphalt mixture increases with the increase of the loading rate, with an approximate logarithmic function. With the increase of temperature, the change trend of failure strength with loading rate becomes more and more gentle. The slope becomes smaller and smaller, and the intercept becomes smaller and smaller. The compression stiffness modulus and the actual loading rate presents a linear increasing trend. The compressive strength of asphalt mixture decreases continuously with the increase of temperature under a certain loading rate. The decreasing range decreases with the increase of temperature, and tends to be gentle when the temperature was high. Furthermore, at the same temperature, the higher the loading rate, the greater the compression failure strength, and the lower the temperature, the more obvious the difference.

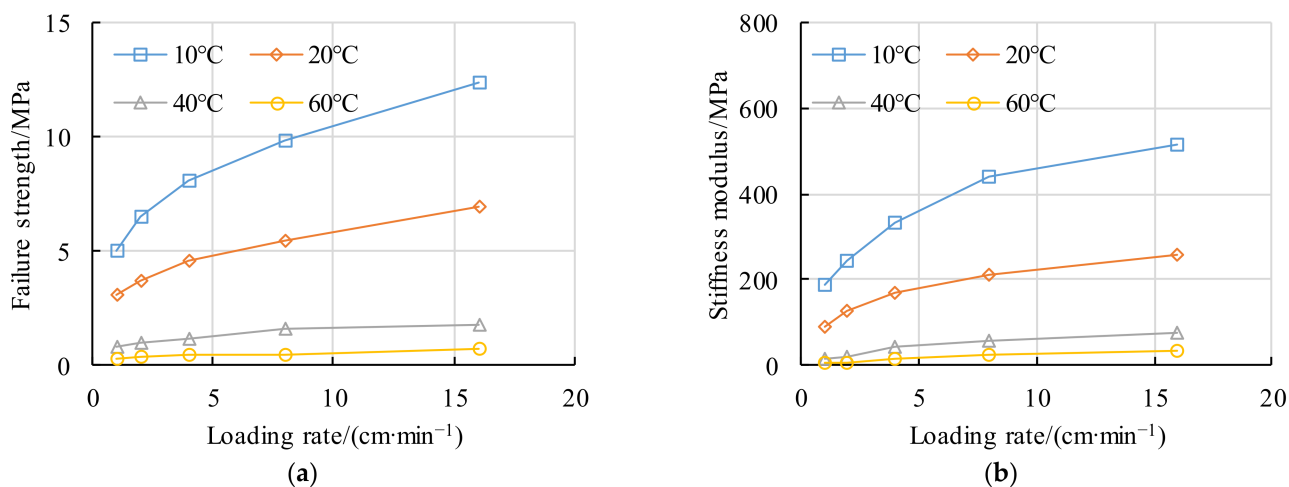


Figure 5. Effect of loading rate and temperature on compression results of 20% CRA mixture: (a) failure strength; (b) stiffness modulus.

3.1.2. Direct Tensile Test

In the tensile test, the mold of the bonded test piece was connected with the loading module through movable bolts, so as to reduce the influence of specimen eccentricity. The influence of CRA content on the direct tensile result of asphalt mixture is shown in Figure 6. The test temperature and loading rate are 20 °C and 4 cm/min respectively. The results showed that, in the initial stage of loading, the load on the specimen increases linearly with the increase of tensile displacement. Then, the slope of the loading curve gradually decreases and tends to be flat, and finally the specimen fractures. Compared with the uniaxial compression test, the strength attenuation of the direct tensile specimen after fracture was more rapid, and the amount of strain required for failure was small. Similarly, it was obvious that the tensile failure stress of asphalt mixture decreases gradually with the increase of CRA content. When the content of CRA was less than 20%, its tensile stress was closer to that of ordinary asphalt mixture. When the content of CRA exceeds 20%, the load associated with failure of asphalt mixture decreases rapidly. This phenomenon was explained as the lower strength of CRA, which makes the asphalt mixture more prone to failure at the aggregate–binder interface. Some studies suggested that, due to the large number of voids in CRA, the thickness of asphalt film around aggregate in the microstructure decreases significantly with the increase in CRA content, which also affects the mechanical properties of asphalt mixture [36].

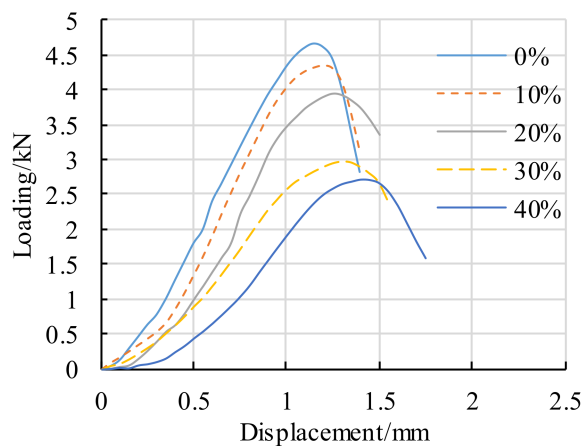


Figure 6. Loading to displacement curves of direct tensile tests.

The influence of temperature and loading rate on the tensile failure of asphalt mixture was shown in Figure 7. The content of CRA in the specimen is 20%. The results showed that the failure strength and stiffness modulus of asphalt mixture decrease with the increase of temperature. This was because the mechanical behavior of asphalt mixture has rheological characteristics. With the increase of temperature, the elastic strength of the material decreases and the visco-plasticity increases. Under the same test temperature, the tensile failure strength of asphalt mixture increases with the increase in loading rate. Compared with compression failure, the increase of loading rate also leads to an increase of the gap in strength and stiffness modulus of tensile failure.

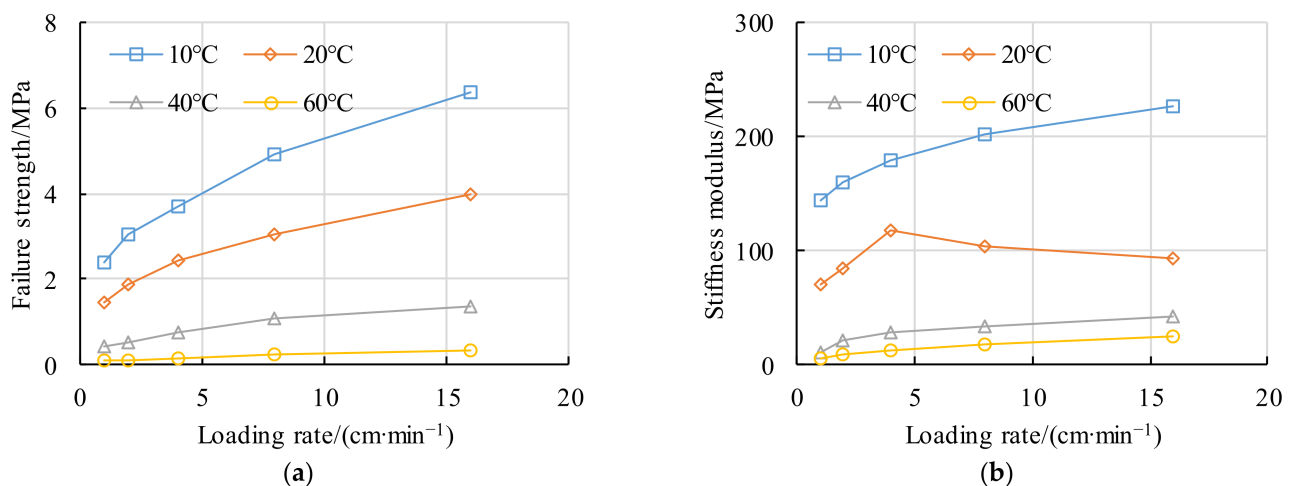


Figure 7. Effect of loading rate and temperature on tensile results of 20% CRA mixture: (a) failure strength; (b) stiffness modulus.

3.1.3. Mohr-Coulomb Strength

According to Mohr-Coulomb theory, when uniaxial compression and direct tensile tests were carried out under the same conditions, the test results can draw the corresponding mole circles to represent the strength of asphalt mixture under different stress states. The cohesive force and internal friction angle of asphalt mixture corresponding to different temperatures and CRA contents were calculated by Equations (2) and (3), as shown in Figure 8.

The results implied that the cohesive force of asphalt mixture increases gradually with the decrease of temperature. The growth rate of cohesive force was very significant. For example, when the temperature was lowered from 40 °C to 20 °C, its cohesive force increases from 0.47 MPa to 1.67 MPa, an increase of more than 2.55 times. However, with the increase of temperature, the internal friction angle descended initially and then increases. This phenomenon indicated that temperature is not the only factor affecting the internal friction angle. From the structural composition, the internal friction force mainly comes from the interlocked denseness of coarse aggregate. Therefore, with the increase of temperature, the performance of asphalt binder was gradually weakened, and the function of coarse aggregate was further enhanced. The results in Figure 8b reveal that CRA plays a significant role in the properties of asphalt mixture (cohesion force and internal friction angle). With the increase of CRA content, the performance of the binder was weakened, and the internal friction angle was gradually smaller due to the edges and corners of the RA being easily broken. It is reasonable to maintain a stable state for the performance of asphalt mixture using 20% CRA instead of fresh aggregates.

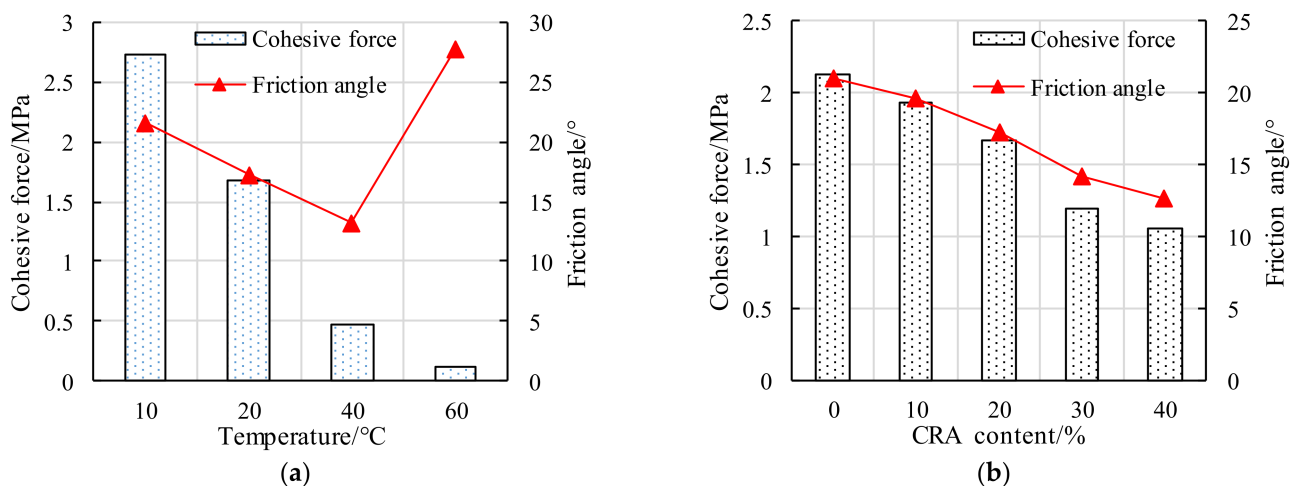


Figure 8. Mohr-Coulomb strength with (a) different temperatures and (b) CRA content.

3.2. Numerical Investigations

The above experimental results were obtained by uniaxial compression and tensile tests using rutted compacted specimens. However, the repeatability of the test results was still hard to guarantee, since the specimens of asphalt mixture are spatially heterogeneous. Previous research suggested that high-precision structural scans could be provided to further explain the influence of component distribution on mechanical properties [13]. This scanning equipment, such as X-ray CT, is generally costly and requires skilled operators. To solve this issue, the DEM model was developed in this study to describe the spatial structure of asphalt mixture using a random field. Meanwhile, the viscoelastic contact model was added to the simulation, and could be used to accurately evaluate the evolution law of the test results.

For the verification of DEM, a wide consensus has been reached in previous studies that all microscopic parameters cannot be obtained by establishing a direct relationship with macroscopic mechanical behavior [37]. Before the numerical test, many attempts were made to adjust the parameters in order to achieve the optimal simulation results in this study. The microscopic parameters of asphalt mixture at 20 °C are shown in Table 4. The details are not described here. Because the random rearrangement of aggregate particles causes the difference in the internal microstructure of the specimen, the mechanical properties of each numerical model were not completely the same. The repeatability of uniaxial compression test and direct tensile test of different specimens could be verified by these DEM models. Five DEM simulations were carried out on asphalt mixture with 20% RCA content. All DEM models have the same material properties and loading conditions. In these models, the spatial distribution of aggregate particles was determined by Gauss function and random number generator. The comparison between the numerical simulation results and the laboratory test is shown in Figure 9, where the loading rate is 4 cm/min.

The results in Figure 9 showed that, for the loading curve, the range of linear stage in the simulation results was larger than that of the experimental results. This was because the numerical model only provides the elastic constitutive model for contacts, and the plastic part of the specimen mainly comes from the compaction process of the voids between particles. With the increase of loading displacement, the contact force between the particles continued to increase. When it reached the limit of stress, contact bonding failed. Then, a large number of micro fractures inside the numerical specimen were marked and tracked. When these micro fractures expanded to penetration, the whole numerical specimen was destroyed, and the force on the loading wall was attenuated sharply. However, after the destruction, the specimen in the experiment still had a certain strength, but suffered from large plastic deformation. This indicated that the role of asphalt binder was always present, whether the specimen was broken or not. The reason for the difference in numerical

results was that DEM was not capable of automatically assigning the bonded mode to new generated contacts. In addition, the comparison of loading results also suggested that the experiment and numerical simulation had good reproducibility under both types of experiment.

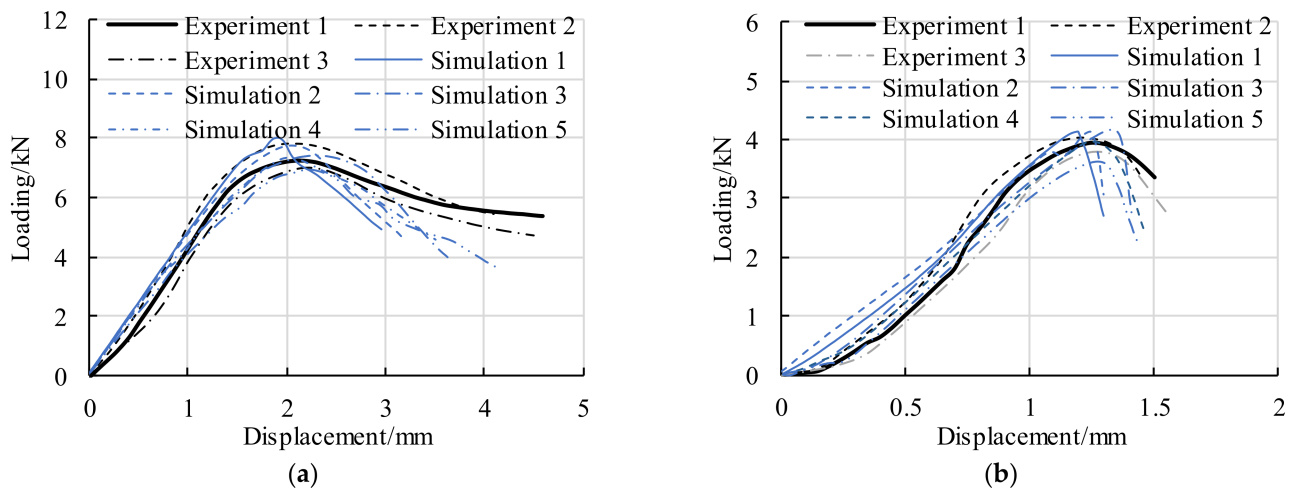


Figure 9. Loading–displacement curves of experiments vs simulations: (a) compression tests and (b) tensile tests.

Further research was carried out to compare the failure strength and stiffness modulus of the two methods, as shown in Figure 10. The average failure strength obtained in the simulation was slightly higher than the experimental result. In compression and tensile tests, the stiffness modulus of the numerical model was equivalent to the results of laboratory tests. At the same time, the error calculated by repeated testing of the numerical model was also within a reasonable limit (less than 15%). It was obvious that the difference in test results caused by the non-uniformity of the internal structure of the specimen was inevitable, and the reliability of the laboratory test and numerical results could be ensured through multiple tests.

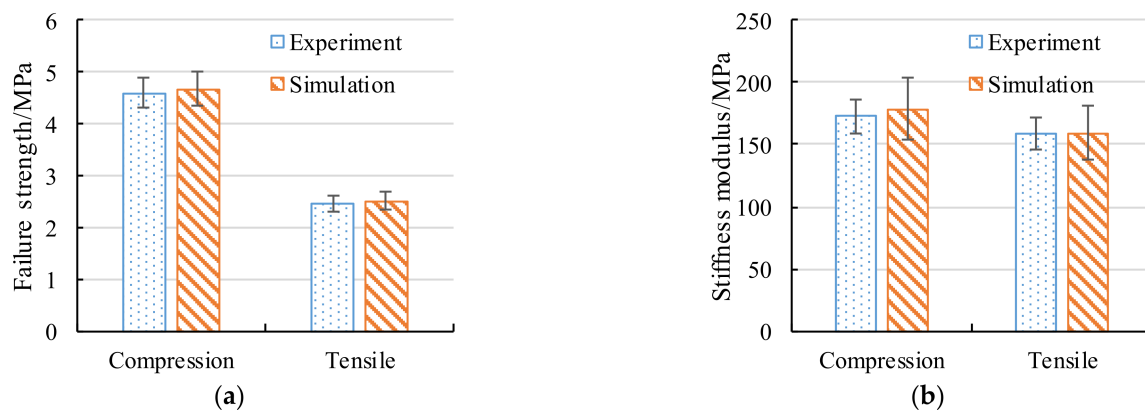


Figure 10. Failure strength and stiffness modulus of experiments vs simulations: (a) compression tests and (b) tensile tests.

The above results proved that DEM provides an effective approach to analyze the mechanical properties of CRA asphalt mixture. Apart from the content of CRA, the property of CRA is also a key factor affecting the failure behavior of asphalt mixture. Based on the numerical model established in this study, the influence of the CRA addition on the performance of asphalt mixture was shown by changing the stiffness ratio of CRA to limestone aggregate and the friction coefficient of contact models. The contact with the CRA connection was given a weak stiffness. Figure 11 illustrates the effect of CRA properties

on Mohr-Coulomb strength. The CRA content in this test is 40%, and the temperature and loading rate are 20 °C and 4 cm/min, respectively. The results showed that, with the decrease of CRA strength, the nominal cohesion force of the specimen decreased, while the internal friction angle increased under loading. The strength of CRA had a strong correlation with the failure performance of asphalt mixture. It was also clear that, when the strength of aggregate was low, the impact of interlocking action between aggregates was more significant on structural properties. The results in Figure 11b implied that the internal friction angle increased with the increase in the friction coefficient. The cohesive force fluctuates within a certain range with the change of the friction coefficient, and its amplitude was small. The reason for this phenomenon was that spherical particles are used to replace irregular aggregates in this study, and the friction coefficient determines the skeleton performance, which causes the cohesive force of the specimen to change accordingly.

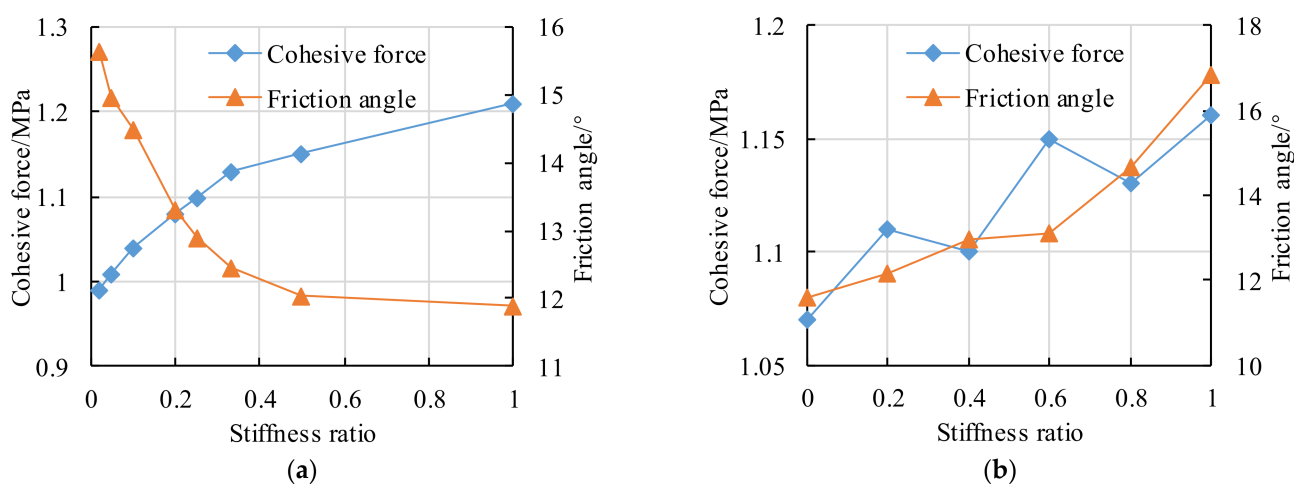


Figure 11. Mohr-Coulomb strength with properties of CRA: (a) stiffness ratio; (b) friction coefficient.

4. Discussion

Due to the combination of fresh aggregate and RA, the total strength of coarse aggregate decreased with the increase of RA content. Moreover, the angular property and abrasion of coarse aggregate also changed with the addition of RA. These properties are closely related to the friction coefficient of particle surface. Therefore, the experimental results with different CRA content indirectly reflect the changes of the above microscopic properties, while the DEM provides an effective tool to further predict the effect of CRA properties on the failure strength of asphalt mixture. Some results and discussion are included as below.

The experimental results showed that the effect of loading rate on the failure strength of the CRA asphalt mixture was substantial, especially when the CRA content was more than 20% and at high temperature. This was because the contact property between asphalt binder and coarse aggregates was weakened because of the presence of cracks and voids on the surface of CRA [38]. The rheology of asphalt binder was more obvious at high temperature. In addition, the CRA content had also a significant influence on the cohesive force and internal friction angle, according to the Mohr-Coulomb theory. Except as the attenuation in the thickness of the asphalt binder, the interlocking action between aggregates also plays a more important role on the failure strength of asphalt mixture at high temperatures.

The distribution and difference of components has an essential influence on the mechanical properties of asphalt mixture. Parallel experiments were conducted to investigate the reproducibility of the results in laboratory and simulation. The comparison in Figures 9 and 10 shows that the failure strength and stiffness modulus had obvious differences in these test specimens with the same composition and properties of materials.

Yu et al. [39] demonstrated that the aggregate segregation during compaction may be an important factor related to the performance of asphalt mixture. In this study, the error limit of failure strength in RAC asphalt mixture is from 5% to 15% due to the spatial variation of aggregate. Therefore, more attempts should be made in future to determine the level of the CRA segregation and its influence on the difference between failure strength.

The DEM simulation in this study was performed taking the stiffness ratio of CRA to fresh aggregate into account. It is obvious that the strength of CRA had a good correlation with the Mohr-Coulomb strength of asphalt mixture. The contact between aggregates was simplified as the sliding friction in the model. Further study should be conducted to establish the DEM model of asphalt mixture using the real aggregate morphology scanned by X-ray CT. In addition, the contribution of coarse and fine aggregates is also an interesting topic to the failure behavior of materials [40]. The current study only described the failure curves under loading, and further study should be conducted on both crack tracks and particle motions microscopically. At last, in order to fully understand the effect of the extreme climate on the mechanical behavior of asphalt mixture, the influence of temperature on the deformation and failure should be made clear by the numerical simulation.

5. Conclusions

This study carried out a laboratory experiment and DEM simulation to investigate the applicability of CRA in asphalt mixture, and the influence of coarse aggregates on the failure strength was taken into account. Both uniaxial compression test and direct tensile test were included. The failure strength of asphalt mixture was determined by Mohr-Coulomb theory. The main findings were as follows.

(1) Temperature and loading rate have a significant influence on the failure strength of asphalt content added by CRA. Along with decrease of temperature, both failure strength and stiffness modulus rapidly enhance. When the temperature was lowered from 40 °C to 20 °C, its cohesive force increased from 0.47 MPa to 1.67 MPa, an increase of more than 2.55 times. Meanwhile, as the loading rate increased, the changes of its failure strength presented a logarithmic upward trend.

(2) CRA content affects the failure properties of asphalt mixture. Along with increase of CRA content, both cohesion force and internal friction angle were gradually weakened. It is applicable to maintain a stable state for the performance of asphalt mixture using 20% CRA instead of fresh aggregates.

(3) The proposed DEM model is a reasonable tool to predict the failure strength of asphalt mixture using CRA. The experimental and simulated specimens yielded highly consistent and repeatable results. The error of repeated tests by random models was less than 15%.

(4) The strength of CRA had a strong correlation with the Mohr-Coulomb strength of asphalt mixture. The simulation showed that, with the decrease of CRA strength, the nominal cohesion force of the specimen decreased, while the internal friction angle increased. Meanwhile, the friction angle of asphalt mixture increased linearly with the friction coefficient of contact models.

Author Contributions: Conceptualization, J.L. and Y.Y.; methodology, Y.Y.; software, J.L.; validation, Y.Y. and C.L.; formal analysis, Y.Y.; investigation, C.L. and X.H.; resources, Y.Y.; data curation, C.L.; writing—original draft preparation, J.L., C.L. and X.H.; writing—review and editing, J.L.; visualization, X.H.; supervision, Y.Y.; project administration, Y.Y.; funding acquisition, Y.Y. All authors have read and agreed to the published version of the manuscript.

Funding: This research was funded by the National Natural Science Foundation of China, grant number 51908562; the Research Foundation of Education Bureau of Hunan Province, China, grant number 19B581; the Natural Science Foundation of Hunan Province, China, grant number 2020JJ5987; the Scientific Research Foundation for the talent introduction of the Central South University of forestry science and technology, grant number 2019YJ033; the Youth Scientific Research Foundation, Central South University of Forestry and Technology, grant number QJ2018008B.

Conflicts of Interest: The authors declare no conflict of interest.

References

1. Wu, Z.; Ann, T.; Shen, L.; Liu, G. Quantifying construction and demolition waste: An analytical review. *Waste Manag.* **2014**, *34*, 1683–1692. [[CrossRef](#)] [[PubMed](#)]
2. Zheng, L.; Wu, H.; Zhang, H.; Duan, H.; Wang, J.; Jiang, W.; Dong, B.; Liu, G.; Zuo, J.; Song, Q. Characterizing the generation and flows of construction and demolition waste in China. *Constr. Build. Mater.* **2017**, *136*, 405–413. [[CrossRef](#)]
3. Aslam, M.S.; Huang, B.; Cui, L. Review of construction and demolition waste management in China and USA. *J. Environ. Manag.* **2020**, *264*, 110445. [[CrossRef](#)] [[PubMed](#)]
4. Wu, S.; Zhong, J.; Zhu, J.; Wang, D. Influence of demolition waste used as recycled aggregate on performance of asphalt mixture. *Road Mater. Pavement Des.* **2013**, *14*, 679–688. [[CrossRef](#)]
5. Cho, Y.-H.; Yun, T.; Kim, I.T.; Choi, N.R. The application of recycled concrete aggregate (RCA) for hot mix asphalt (HMA) base layer aggregate. *KSCE J. Civ. Eng.* **2011**, *15*, 473–478. [[CrossRef](#)]
6. Martinho, F.; Picado-Santos, L.; Capitão, S. Feasibility assessment of the use of recycled aggregates for asphalt mixtures. *Sustainability* **2018**, *10*, 1737. [[CrossRef](#)]
7. Fatemi, S.; Imaninasab, R. Performance evaluation of recycled asphalt mixtures by construction and demolition waste materials. *Constr. Build. Mater.* **2016**, *120*, 450–456. [[CrossRef](#)]
8. Arabani, M.; Moghadas Nejad, F.; Azarhoosh, A. Laboratory evaluation of recycled waste concrete into asphalt mixtures. *Int. J. Pavement Eng.* **2013**, *14*, 531–539. [[CrossRef](#)]
9. Song, W.; Xu, Z.; Xu, F.; Wu, H.; Yin, J. Fracture investigation of asphalt mixtures containing reclaimed asphalt pavement using an equivalent energy approach. *Eng. Fract. Mech.* **2021**, *253*, 107892. [[CrossRef](#)]
10. Behnia, B.; Dave, E.V.; Ahmed, S.; Buttlar, W.G.; Reis, H. Effects of recycled asphalt pavement amounts on low-temperature cracking performance of asphalt mixtures using acoustic emissions. *Transp. Res. Rec.* **2011**, *2208*, 64–71. [[CrossRef](#)]
11. Huang, Q.; Qian, Z.; Hu, J.; Zheng, D.; Chen, L.; Zhang, M.; Yu, J. Investigation on the properties of aggregate-mastic interfacial transition zones (ITZs) in asphalt mixture containing recycled concrete aggregate. *Constr. Build. Mater.* **2021**, *269*, 121257. [[CrossRef](#)]
12. Guo, Q.; Chen, Z.; Liu, P.; Li, Y.; Hu, J.; Gao, Y.; Li, X. Influence of basalt fiber on mode I and II fracture properties of asphalt mixture at medium and low temperatures. *Theor. Appl. Fract. Mech.* **2021**, *112*, 102884. [[CrossRef](#)]
13. Wei, H.; Li, J.; Wang, F.; Zheng, J.; Tao, Y.; Zhang, Y. Numerical investigation on fracture evolution of asphalt mixture compared with acoustic emission. *Int. J. Pavement Eng.* **2021**, 1–11. [[CrossRef](#)]
14. Lu, D.X.; Nguyen, N.H.; Saleh, M.; Bui, H.H. Experimental and numerical investigations of non-standardised semi-circular bending test for asphalt concrete mixtures. *Int. J. Pavement Eng.* **2021**, *22*, 960–972. [[CrossRef](#)]
15. Guo, Q.; Wang, H.; Gao, Y.; Jiao, Y.; Liu, F.; Dong, Z. Investigation of the low-temperature properties and cracking resistance of fiber-reinforced asphalt concrete using the DIC technique. *Eng. Fract. Mech.* **2020**, *229*, 106951. [[CrossRef](#)]
16. Liu, C.; Lv, S.; Jin, D.; Qu, F. Laboratory investigation for the road performance of asphalt mixtures modified by rock asphalt-styrene butadiene rubber. *J. Mater. Civ. Eng.* **2021**, *33*, 04020504. [[CrossRef](#)]
17. Qin, X.; Ma, L.; Wang, H. Comparison analysis of dynamic modulus of asphalt mixture: Indirect tension and uniaxial compression test. *Transp. A: Transp. Sci.* **2019**, *15*, 165–178. [[CrossRef](#)]
18. Cerni, G.; Bocci, E.; Cardone, F.; Corradini, A. Correlation between asphalt mixture stiffness determined through static and dynamic indirect tensile tests. *Arab. J. Sci. Eng.* **2017**, *42*, 1295–1303. [[CrossRef](#)]
19. Lv, S.; Liu, C.; Chen, D.; Zheng, J.; You, Z.; You, L. Normalization of fatigue characteristics for asphalt mixtures under different stress states. *Constr. Build. Mater.* **2018**, *177*, 33–42. [[CrossRef](#)]
20. Zhang, J.; Li, J.; Yao, Y.; Zheng, J.; Gu, F. Geometric anisotropy modeling and shear behavior evaluation of graded crushed rocks. *Constr. Build. Mater.* **2018**, *183*, 346–355. [[CrossRef](#)]
21. Qian, G.; Hu, K.; Li, J.; Bai, X.; Li, N. Compaction process tracking for asphalt mixture using discrete element method. *Constr. Build. Mater.* **2020**, *235*, 117478. [[CrossRef](#)]
22. Shaheen, M.; Al-Mayah, A.; Tighe, S. A novel method for evaluating hot mix asphalt fatigue damage: X-ray computed tomography. *Constr. Build. Mater.* **2016**, *113*, 121–133. [[CrossRef](#)]
23. Chen, J.; Huang, B.; Shu, X. Air-void distribution analysis of asphalt mixture using discrete element method. *J. Mater. Civ. Eng.* **2013**, *25*, 1375–1385. [[CrossRef](#)]
24. Ma, T.; Zhang, D.; Zhang, Y.; Wang, S.; Huang, X. Simulation of wheel tracking test for asphalt mixture using discrete element modelling. *Road Mater. Pavement Des.* **2018**, *19*, 367–384. [[CrossRef](#)]
25. Zelelew, H.M.; Papagiannakis, A.T. Micromechanical modeling of asphalt concrete uniaxial creep using the discrete element method. *Road Mater. Pavement Des.* **2010**, *11*, 613–632. [[CrossRef](#)]
26. Chen, M.; Wong, Y. Evaluation of the development of aggregate packing in porous asphalt mixture using discrete element method simulation. *Road Mater. Pavement Des.* **2017**, *18*, 64–85. [[CrossRef](#)]
27. Al Khateeb, L.; Anupam, K.; Erkens, S.; Scarpas, T. Micromechanical simulation of porous asphalt mixture compaction using discrete element method (DEM). *Constr. Build. Mater.* **2021**, *301*, 124305. [[CrossRef](#)]

28. Song, W.; Xu, F.; Wu, H.; Xu, Z. Investigating the skeleton behaviors of open-graded friction course using discrete element method. *Powder Technol.* **2021**, *385*, 528–536. [[CrossRef](#)]
29. Feng, H.; Pettinari, M.; Stang, H. Study of normal and shear material properties for viscoelastic model of asphalt mixture by discrete element method. *Constr. Build. Mater.* **2015**, *98*, 366–375. [[CrossRef](#)]
30. Rafi, M.M.; Qadir, A.; Ali, S.; Siddiqui, S.H. Performance of hot mix asphalt mixtures made of recycled aggregates. *J. Test. Eval.* **2014**, *42*, 357–367. [[CrossRef](#)]
31. Code of China. *Standard Test Methods of Bitumen and Bituminous Mixtures for Highway Engineering*; JTG E20—2011; Code of China: Beijing, China, 2011.
32. Jin, J.; Gao, Y.; Wu, Y.; Li, R.; Liu, R.; Wei, H.; Qian, G.; Zheng, J. Performance evaluation of surface-organic grafting on the palygorskite nanofiber for the modification of asphalt. *Constr. Build. Mater.* **2021**, *268*, 121072. [[CrossRef](#)]
33. Jin, J.; Gao, Y.; Wu, Y.; Liu, S.; Liu, R.; Wei, H.; Qian, G.; Zheng, J. Rheological and adhesion properties of nano-organic palygorskite and linear SBS on the composite modified asphalt. *Powder Technol.* **2021**, *377*, 212–221. [[CrossRef](#)]
34. Yao, Y.; Ni, J.; Li, J. Stress-dependent water retention of granite residual soil and its implications for ground settlement. *Comput. Geotech.* **2021**, *129*, 103835. [[CrossRef](#)]
35. Li, J.; Zhang, J.; Qian, G.; Zheng, J.; Zhang, Y. Three-dimensional simulation of aggregate and asphalt mixture using parameterized shape and size gradation. *J. Mater. Civ. Eng.* **2019**, *31*, 04019004. [[CrossRef](#)]
36. Li, P.; Jiang, X.; Ding, Z.; Zhao, J.; Shen, M. Analysis of viscosity and composition properties for crumb rubber modified asphalt. *Constr. Build. Mater.* **2018**, *169*, 638–647. [[CrossRef](#)]
37. Wang, X.; Nie, Z.; Gong, J.; Liang, Z. Random generation of convex aggregates for DEM study of particle shape effect. *Constr. Build. Mater.* **2021**, *268*, 121468. [[CrossRef](#)]
38. Li, P.; Su, J.; Ma, S.; Dong, H. Effect of aggregate contact condition on skeleton stability in asphalt mixture. *Int. J. Pavement Eng.* **2020**, *21*, 196–202. [[CrossRef](#)]
39. Yu, H.; Yang, M.; Qian, G.; Cai, J.; Zhou, H.; Fu, X. Gradation segregation characteristic and its impact on performance of asphalt mixture. *J. Mater. Civ. Eng.* **2021**, *33*, 04020478. [[CrossRef](#)]
40. Yao, Y.; Li, J.; Ni, J.; Liang, C.; Zhang, A. Effects of gravel content and shape on shear behaviour of soil-rock mixture: Experiment and DEM modelling. *Comput. Geotech.* **2022**, *141*, 104476.